Continuum-discretized coupled-channels method for four-body breakup reactions *

M. Kamimura[1], T. Matsumoto[1], E. Hiyama[2], K. Ogata[1], Y. Iseri[3], and M. Yahiro[1]

[1]*Department of Physics, Kyushu University, Fukuoka 812-8581, Japan*

[2]*Department of Physics, Nara Women's University, Nara 630-8506, Japan and*

[3]*Department of Physics, Chiba-Keizai College, Chiba 263-0021, Japan*

(Dated: February 9, 2008)

Development of the method of CDCC (Continuum-Discretized Coupled-Channels) from the level of three-body CDCC to that of four-body CDCC is reviewed. Introduction of the pseudo-state method based on the Gaussian expansion method for discretizing the continuum states of two-body and three-body projectiles plays an essential role in the development. Furthermore, introduction of the complex-range Gaussian basis functions is important to improve the CDCC for nuclear breakup so as to accomplish that for Coulomb and nuclear breakup. A successful application of the four-body CDCC to ^{6}He+^{12}C scattering at 18 and 229.8 MeV is reported.

I. INTRODUCTION

In the study of reactions induced by unstable nuclei, analysis of the case where the projectile is considered to be composed of three-clusters such as ^{6}He and ^{11}Li becomes quite important. For this purpose, along the diagram in Fig. 1, we have developed the three-body CDCC (Continuum-Discretized Coupled-Channels) for nuclear breakup of two-body projectiles [1] into the four-body CDCC for Coulomb and nuclear breakup of three-body projectiles.

The momentum-bin method to discretize the continuum states of the two-body projectiles (such as $^6\mathrm{Li} = \alpha + d$, $^8\mathrm{B} + p$, etc.) is not practically available to the case of three-body projectiles. On the basis of the Gaussian expansion method (GEM)[2], we proposed, in Ref.[3], the pseudo-state (PS) method to discretize the continuum states and examined it in the case of two-body projectiles (three-body CDCC); this is Step A in Fig.1. In the PS method we diagonalized the two-body Hamiltonian of the internal motion of the projectile using the Gaussian basis functions [2] and obtained dense distribution of the pseudo-states, namely discretized continuum states. An advantage of this method is that it can easily be extended to the case of three-body projectiles by using the GEM. Another advantage of the PS method is that we can derive continuous S-matrix elements as a smooth function of the momentum of the projectile breakup states. We found [3] that the S-matrix elements

* A talk given at the Workshop on Reaction Mechanisms for Rare Isotope Beams, Michigan State University, March 9-12, 2005 (to appear in an AIP Conference Proceedings).

obtained by the PS method agrees well with the S-matrix elements by the momentum-bin method with very precise bins.

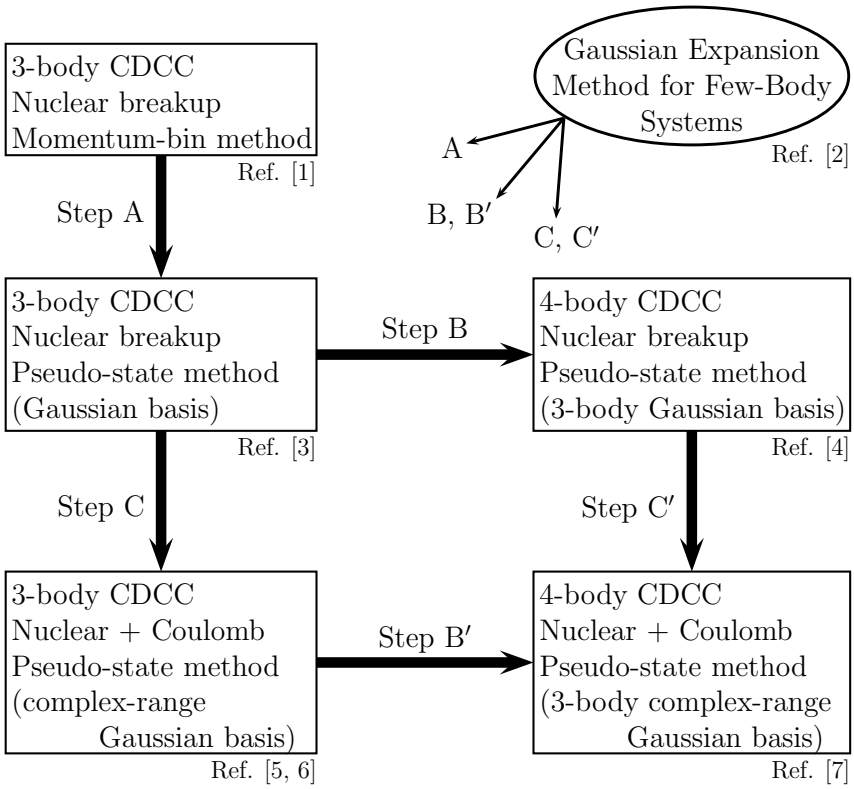

FIG. 1: A flow of the improvement of the method of CDCC starting from the three-body CDCC for nuclear breakup to the four-body CDCC for Coulomb and nuclear breakup with the aid of the Gaussian expansion method for few-body systems.

As Step B in Fig.1, we extended the three-body CDCC (for nuclear breakup) to the four-body CDCC (for nuclear breakup) using the three-body Gaussian basis functions of GEM to obtain bound and pseudo-states of the three-body projectiles [4]. The GEM is very suitable for describing bound and pseudo-states of three- and four-body systems; it is extensively reviewed in Ref.[2]. The four-body CDCC was applied to the ^{6}He+^{12}C at 18 and 229.8 MeV. The differential cross sections of the elastic scattering were well reproduced by using the double-folding CC potentials.

In Step C, we improved the three-body CDCC for nuclear breakup to that for Coulomb and nuclear breakup [5] by using the PS method with the complex-range Gaussian basis functions [2] instead of the (real-range) Gaussian basis functions adopted in the previous Steps. Due to the long-ranged Coulomb coupling-potentials, the modelspace required for CDCC is very large. Particularly, one must prepare the internal wave functions of the projectile, both in bound and continuum states, for a wide range of the internal coordinate, say 0–100 fm, which is in general difficult for PS methods. This can easily be achieved by using the complex-range Gaussian basis in the case of two-body projectile.

In order to treat both Coulomb and nuclear breakup processes at *intermediate energies* with high accuracy and computational speed, a new method was proposed in Ref. [6];

namely, a hybrid calculation with the three-body CDCC method and the eikonal-CDCC (E-CDCC) method. E-CDCC describes the center-of-mass motion of the projectile relative to the target by straight-line approximation (or by using Coulomb wave functions instead of plane waves) and treats the excitation of the projectile explicitly by CDCC with the momentum-bin method or the PS method. E-CDCC drastically reduces computation time and eliminates many problems concerned with huge angular momentum in solving coupled-channel equations. Thus, the hybrid calculation is expected to be opening the door to the systematic analysis of Coulomb (plus nuclear) dissociation of projectiles in the wide range of beam energies.

Finally, by Step B' (or by Step C') we can reach the four-body CDCC for Coulomb and nuclear breakup. This step was not reported in the time of the RIA workshop but was recently accomplished and successfully applied to the ^{6}He+^{209}Bi scattering at 19.0 and 22.5 MeV [7].

II. METHOD OF PSEUDO-STATE CDCC FOR TWO-BODY PROJECTILES

In the method of CDCC, the total wave function of the scattering state Ψ_{JM} is expanded in terms of a finite number of internal wave functions $\Psi_{nIm}(\xi)$ of the projectile:

$$\Psi^{JM}(\xi, \mathbf{R}) = \sum_{nI,L} [\Phi_{nI}(\xi) \otimes \chi^J_{nI,L}(\mathbf{R})]_{JM}, \tag{2.1}$$

where $\mathbf{R}$ is the coordinate of the center-of-mass of the projectile relative to the target, and ξ is the internal coordinates of the projectile. I is the total spin of the projectile and n stands for the nth eigenstate. $\chi^J_{nI,L}$ represents the relative motion between the projectile and the target; L is the orbital angular momentum regarding $\mathbf{R}$. The unknown function $\chi^J_{nI,L}(\mathbf{R})$ are solved using the usual framework of the coupled-channel method for discrete excited states.

The projectile internal wave functions $\Phi_{nI}(\xi)$ include both bound states and discretized continuum states. To calculate the wave functions of the latter states the momentum-bin method has widely been utilized in the usual three-body CDCC calculations. In the method the exact scattering wave functions are averaged within each narrow intervals of momentum between the two constituents in the projectile. But, this method is not practically suitable for discretizing the breakup states of the three-body projectile.

In the pseudo-state (PS) method [1, 8, 9], on the other hand, wave functions of the discretized breakup states are obtained by diagonalizing the internal Hamiltonian of the projectile, which describes the relative motion of the two constituents, using L^2-type basis functions. Since the wave functions of such pseudo breakup states have wrong asymptotic forms, the PS method was mainly used in the past to describe virtual breakup processes in the intermediate stage of elastic scattering [9] and (d, p) reactions [1].

In the work of Ref.[3], however, we proposed the new method of pseudo-state (PS) discretization for two-body projectiles. It can be used not only for virtual breakup processes in elastic scattering but also for breakup reactions. In order to diagonalize the Hamiltonian of the two-body projectile, we employed two types of basis functions. One is the conventional

real-range Gaussian functions

$$\phi_{j\ell}(r) = r^\ell \exp\left[-(r/a_j)^2\right], \qquad (j = 1\text{–}n) \tag{2.2}$$

where $\{a_j\}$ are assumed to increase in a geometric progression [2, 10]:

$$a_j = a_1 (a_n/a_1)^{(j-1)/(n-1)}. \tag{2.3}$$

The other is an extension of (2.2) introduced in Ref. [2], i.e., the following pairs of functions:

$$\begin{aligned} \phi^{\rm C}_{j\ell}(r) &= r^\ell \exp\left[-(r/a_j)^2\right] \cos\left[b\,(r/a_j)^2\right], \\ \phi^{\rm S}_{j\ell}(r) &= r^\ell \exp\left[-(r/a_j)^2\right] \sin\left[b\,(r/a_j)^2\right], \quad (j = 1\text{–}n). \end{aligned} \tag{2.4}$$

Here, b is a free parameter, in principle, but numerical test showed that $b = \pi/2$ is recommendable. Both $\phi^{\rm C}_{j\ell}$ and $\phi^{\rm S}_{j\ell}$ are to be used simultaneously; the total number of basis is thus $2n$. The basis functions (2.4) can also be expressed as

$$\begin{aligned} \phi^{\rm C}_{j\ell}(r) &= \{\psi^*_{j\ell}(r) + \psi_{j\ell}(r)\}/2, \\ \phi^{\rm S}_{j\ell}(r) &= \{\psi^*_{j\ell}(r) - \psi_{j\ell}(r)\}/(2i), \end{aligned} \tag{2.5}$$

with

$$\psi_{j\ell}(r) = r^\ell \exp[-\eta_j r^2], \quad \eta_j = (1 + i\,b)/a_j^2, \tag{2.6}$$

i.e., Gaussian functions with a complex-range parameter. We thus refer to the basis $\phi^{\rm C}_{j\ell}$ and $\phi^{\rm S}_{j\ell}$ as the complex-range Gaussian basis.

The complex-range Gaussian basis functions are oscillating with r. They are therefore expected to simulate the oscillating pattern of the continuous breakup state wave functions better than the real-range Gaussian basis functions do. Moreover, numerical calculation with the complex-range Gaussians can be done using essentially the same computer programs as for the real-range Gaussians, just replacing real variables for a_j of Eq. (2.3) by complex ones. Usefulness of the real- and complex-range Gaussian basis functions in few-body calculations are extensively presented in the review work [2].

Here, we explore a typical example in which the complex-range Gaussian basis functions reproduce highly oscillatory functions with high accuracy. A good test is to calculate the wave functions of highly excited states in a harmonic oscillator potential; note that this potential is not specially advantageous for the Gaussian bases. We take the case of a nucleon with angular momentum $l = 0$ in a potential having $\hbar\omega = 15.0$ MeV. Parameters of the complex-range Gaussian basis functions are $\{\, 2n = 28, a_1 = 1.4\,\text{fm}, a_n = 5.8\,\text{fm}, b = \frac{\pi}{2}\frac{1}{1.2^2} = 1.09\,\}$. For the sake of comparison, we also tested the Gaussian basis functions with the parameters $\{n = 28,\ a_1 = 0.5\,\text{fm},\ a_n = 11.3\,\text{fm}\ \}$. Optimized a_1 and a_n are quite different between the two types of bases though the total numbers of basis functions are the same. In Table 1, we compare the calculated energy eigenvalues with the exact ones. It is evident that the complex-range Gaussians can reproduce the energy up to much more highly excited states than the Gausssians do. For the Gaussian basis, even if the number of basis functions is increased, the result is not significantly improved, because the number of oscillation does

TABLE I: Test of the accuracy of real-range and complex-range Gaussian basis functions for highly excited states ($2n + l \leq 46$, $l = 0$) of a harmonic oscillator potential for a nucleon. The number of basis functions is 28 for both cases. Eigenenergies obtained by the diagonalization of the Hamiltonian with the bases are listed in terms of the number of quanta, $E/\hbar\omega - \frac{3}{2}$. See text for the Gaussian parameters.

Exact (2n)	**real range**	**complex range**	**Exact (2n)**	**real range**	**complex range**
0.0	0.0000	0.0000	26.0	26.4	26.0001
6.0	6.0000	6.0000	30.0	32.9	30.0003
10.0	10.0000	10.0000	34.0	41.8	34.002
14.0	14.0000	14.0000	38.0	53.8	38.003
18.0	17.998	18.0000	42.0	69.9	42.1
22.0	21.9	22.0000	46.0	91.6	46.3

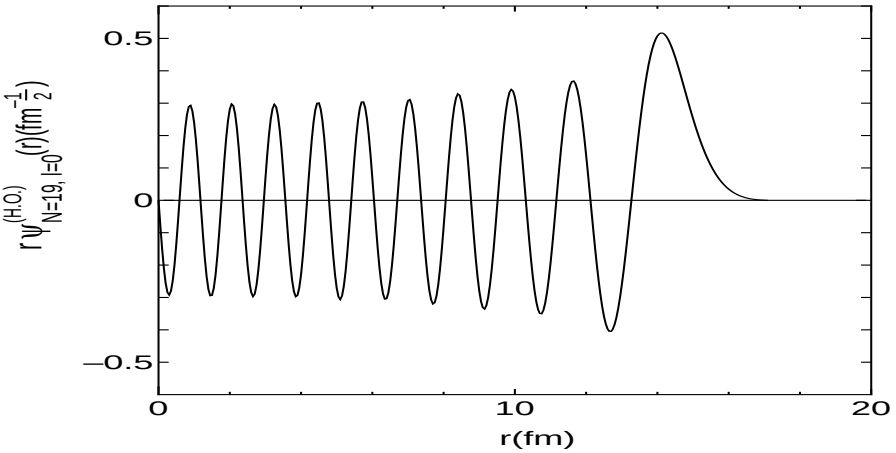

FIG. 2: Accuracy of the wave function of the $2n + l = 38$, $l = 0$ state obtained by diagonalizing Hamiltonian with a harmonic-oscillator potential for a nucleon using 28 complex-range Gaussian basis functions. It is compared with the exact wave function but the difference is invisible since the error is less than a few % everywhere. See text for the Gaussian parameters. This figure is taken from Ref. [2].

not increase. On the other hands, for the complex-range Gaussian functions, as the number is increased, the result becomes better so long as the number of oscillation is not too larger than ~ 20. Figure 2 demonstrates good accuracy of the wave function of the 19-th excited state having 38 quanta. Error is within a few %, much smaller than the thickness of the line. The figure suggests that the basis functions is also suitable for describing pseudo-states used for Coulomb breakup reactions.

We here emphasize that even in the case where the projectile is assumed to be three-body

system, the Gaussian basis functions with real and complex ranges are easily utilized in the CDCC calculation with the PS method. We discuss this point in the next section.

Another advantage of the PS method, in the case of two-body projectiles, is that the discrete breakup S-matrix elements, say $S_{nIL,0I_0L_0}$, for the transition from $\Phi_{0I_0}(\xi)$ to $\Phi_{nI}(\xi)$ can be accurately transformed to smooth S-matrix elements, say $\tilde{S}_{IL,I_0L_0}(k)$, as following [3], since the two-body PS basis functions can form in the good approximation a complete set in the finite region which is important for the breakup processes:

$$\tilde{S}_{IL,0I_0L_0}(k) = \sum_n \langle \tilde{\Phi}_I(k,\xi)|\Phi_{nI}(\xi)\rangle_\xi \; S_{nIL,0I_0L_0} \; , \tag{2.7}$$

where $\tilde{\Phi}_I(k,\xi)$ is the exact wave function of the internal motion of the two-body projectile.

Example 1 : ^{6}Li+^{40}C scattering at 156 MeV.

Here, we briefly show results of test calculations done in [3] ^{6}Li+^{40}C scattering at 156 MeV. The $\alpha - d$ continuum of the ^{6}Li projectile is discretized as in Fig. 3 using the real-range Gaussian bases and the complex-range Gaussian bases. The modelspace sufficient for describing breakup processes in this scattering is $k_{\max} = 2.0$ fm^{-1} and $\ell_{\max} = 2$; the modelspace is composed of two k-continua for s-state and d-state. There exists a d-state resonance. The resonance is automatically taken care by the PS method by the lowest-lying several pseudo-states. On the other hand, in the momentum-bin method, the d-state k-continuum is further divided in the momentum-bin method into the resonant part [$0 < k < 0.55\,\mathrm{fm}^{-1}$] and the non-resonant part [$0.55 < k < 2.0\,\mathrm{fm}^{-1}$]. In the former region the k continuum d-state wave function varies rapidly with k. The momentum-bin method can simulate this rapid change with bins of an extremely small width. In fact clear convergence is found for both the elastic and the breakup S-matrix elements, when the resonance part is described by 30 bins and the non-resonance part of the d-state and the s-state k-continua by 20 bins.

Figure 4 represents breakup S-matrix elements at grazing total angular momentum $J = 43$; (a) s-state breakup and (b) d-state breakup in the case of $L = J - 2$. The real- and complex-range Gaussian PS discretization well reproduce the "exact" solution calculated by the momentum-bin method with dense bins. The results of the two PS methods turn out to coincide within the thickness of the line. The resonance peak can be expressed by only 8 (12) breakup channels in the complex-range (real-range) Gaussian PS method, while the corresponding number of breakup channels is 30 in the momentum-bin method, as mentioned above. Thus, one can conclude that the real- and complex-range Gaussian PS methods are very useful for describing not only non-resonant states but also resonant ones.

The PS method has at least two advantages over the widely used momentum bin average method. One is that it does not need the exact wave function of the projectile over the entire region of r. This is important from a theoretical point of view. The other is that with the real- and complex-range Gaussian bases one can calculate all the coupling potentials semi-analytically [2], which is very useful in actual calculations; note that the Gaussian bases are very suitable for transforming wave functions and interactions from a Jacobian coordinate system to other ones. Furthermore, if the projectile has resonances in its excitation spectrum,

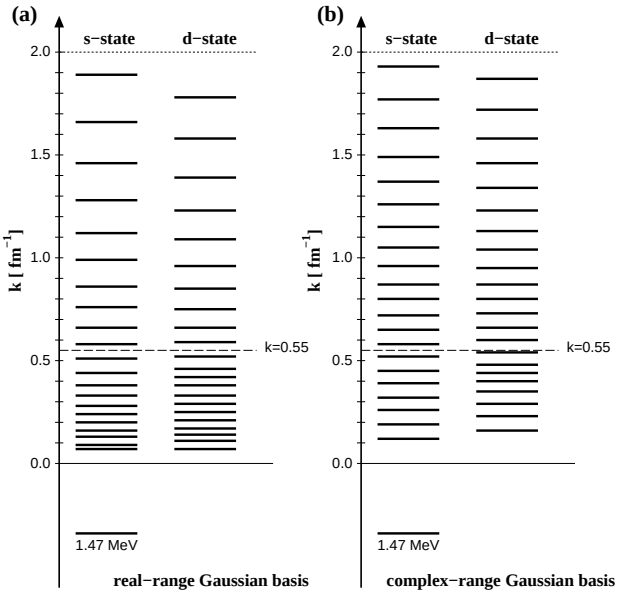

FIG. 3: Pseudo states (discretized continuum states) for ^{6}Li obtained by using the real-range Gaussian basis functions (left) and the complex-range Gaussian basis functions (right). This figure is taken from Ref.[3].

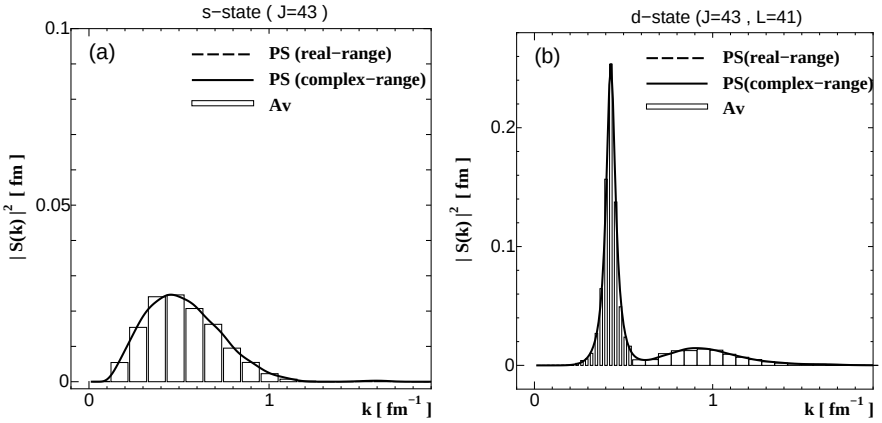

FIG. 4: The squared moduli of breakup S-matrix elements as a function of k at the grazing total angular momentum $J = 43$ for ^{6}Li + ^{40}Ca scattering at 156 MeV. The step line is the result of the momentum-bin method (Average-method) with dense bins. s-state breakup (left) and d-state breakup for $L = J-2$ (right). Note that the difference between the results of the real- and complex-range Gaussian PS methods is not visible since it is less than about 1%. This figure is taken from Ref.[3].

the PS method discretizes the complicated spectrum with a reasonable number of the pseudo-states, without distinguishing the resonance states from non-resonant continuous states. These advantages of the PS method are extremely helpful, sometimes even essential, in applying CDCC to four-body breakup effects of unstable nuclei such as ^{6}He and ^{11}Li.

Example 2 : ^{8}B+^{58}Ni scattering at 25.8 MeV.

Here, we briefly show results of test calculation in [5] for Coulomb breakup process of ^{8}B+^{58}Ni scattering at 25.8 MeV. The ^{7}Be$-p$ continuum in the ^{8}B projectile is discretized

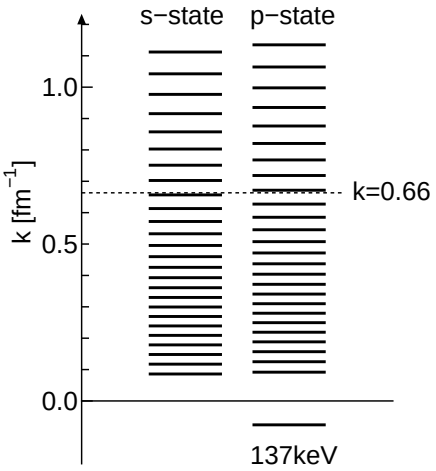

FIG. 5: Discretized momenta for ^{8}B; the left (right) side corresponds to the s-state (p-state). The horizontal dotted line represents the cutoff momentum $k_{\max}$ taken to be 0.66 fm^{-1} above which is not effective in the reaction. This figure is taken from Ref.[5].

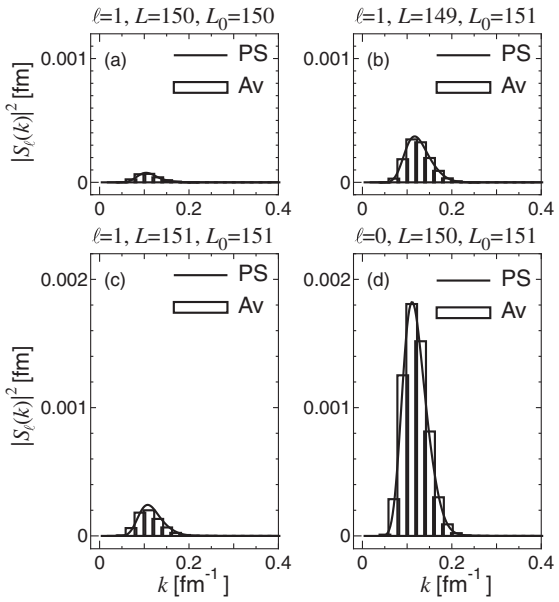

FIG. 6: The squared moduli of breakup S-matrix elements, as a function of k, at $J = 150$ for ^{8}B+^{58}Ni scattering at 25.8 MeV. The panel (a), (b), (c) and (d) correspond to $(\ell, L, L_0) = (1, 150, 150)$, (1,149,151), (1,151,151) and (0,150,151), respectively. In each panel, the solid line represents the result of PS-CDCC, while the step line is the result of the momentum-bin (average) method of CDCC that is assumed as the "exact" S-matrix elements. This figure is taken from Ref.[5].

as in Fig. 5 by the PS method with the real-range Gaussian bases and the complex-range Gaussian bases. In the PS method, the number of channels included in the CDCC calculation, was 18 for both the s- and p-states at $k < k_{\max} = 0.66$ fm^{-1}, which give a satisfactory convergence of the result. The resulting wave functions with positive eigenenergies turned out to oscillate up to about 100 fm. In the momentum-bin method, the modelspace with $k_{\max} = 0.66$ fm^{-1} and $\Delta k = 0.66/16$ $(0.66/32)$ fm^{-1} for p-state (s-state) gives convergence of the resulting total breakup cross section. The maximum internal coordinate $r_{\max}$ was taken to be 100 fm.

Figure 6 shows the result of the comparison of $|S_\ell(k)|^2$ at $J = 150$, which corresponds to the scattering angle of 10° assuming the classical path. It was found that CDCC calculation with only Coulomb coupling potentials gives a peak at 10° in the total breakup cross section. Thus, it can be assumed that Fig. 6 corresponds to the most-Coulomb-like breakup process; in any case, the feature of the result was found to be almost independent of J. In each panel of Fig. 6, one sees that the result of PS-CDCC (solid line) very well reproduces the "exact" solution (step line by the momentum-bin method) for all k being significant for the ^{8}B Coulomb breakup.

III. GAUSSIAN EXPANSION METHOD FOR FEW-BODY SYSTEMS

In this section we briefly explain the Gaussian expansion method (GEM) for few-body systems. The method was proposed by Kamimura in 1988 [10] for three-body systems and was much developed by Hiyama using the infinitesimally-shifted Gaussian basis functions even for four-body systems (reviewed in [2]).

A good example to show the accuracy and usefulness of the method is the determination of upper limit of the difference between the masses of proton and antiproton, m_p and $m_{\bar{p}}$, respectively. The first recommended upper limit of $|m_{\bar{p}} - m_p|/m_p$ by the Particle Data Group listed in Particle Listings 2000 [11] was 5×10^{-7}, which could be used for a test of CPT invariance. This number was extracted from a high-resolution laser experiment involving metastable states of antiprotonic helium atom ($\mathrm{He}^{2+} + e^- + \bar{p}$) [12] by Kino *et al.* [13] through a theoretical analysis of the highly excited states of the Coulomb three-body system using GEM. The ratio was improved to $|m_{\bar{p}} - m_p|/m_p < 1 \times 10^{-8}$, as listed in the Particle Listings 2004, by later, more extensive experiments and additional calculations (cf. Ref.[2])

In the Gaussian expansion method [2], wave functions of the projectile, Φ_{nIm} in (2.1), is written as a sum of component functions in the Jacobian coordinates for rearrangement channels $c = 1 - 3$ in Fig. 7 as

$$\Phi_{nIm}(\xi) = \sum_{c=1}^{3} \psi^{(c)}_{nIm}(\xi), \tag{3.1}$$

Each $\psi^{(c)}_{nIm}$ is expanded in terms of the Gaussian basis functions:

$$\psi^{(c)}_{nIm}(\xi) \;=\; \varphi^{(\alpha)} \sum_{\lambda\ell\Lambda S} \sum_{i=1}^{i_{\max}} \sum_{j=1}^{j_{\max}} A^{(c)nI}_{i\lambda j\ell\Lambda S}\; y_c^\lambda\, r_c^\ell\, e^{-(y_c/\bar{y}_i)^2}\, e^{-(r_c/\bar{r}_j)^2}$$

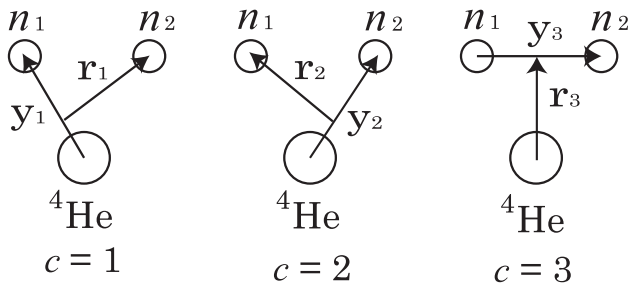

FIG. 7: Jacobian coordinates of three rearrangement channels ($c = 1$–3) adopted for the n+n+^{4}He model of ^{6}He structure. The two neutrons are to be antisymmetrized.

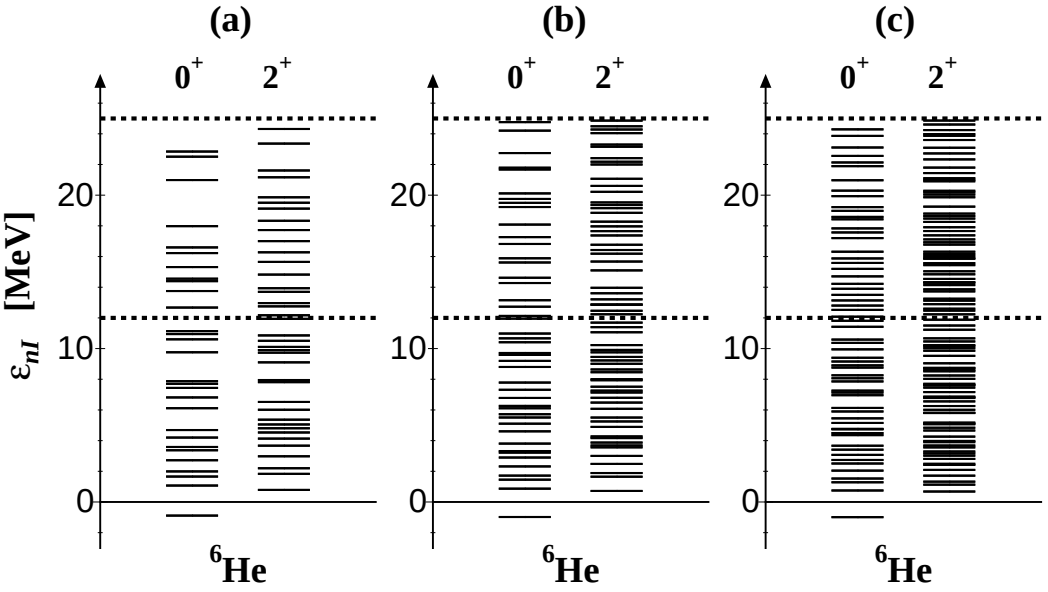

FIG. 8: Calculated energy levels of the bound and discretized continuum states (pseudo-states) of ^{6}He using three different sets of Gaussian basis functions (see Ref. [4]). The numbers of the pseudo-states used in the ^{6}He+^{12}C scattering at 229.8 MeV to see convergence of the calculated results is (a) 28 (0^+) and 39 (2^+), (b) 44 (0^+) and 64 (2^+) and (c) 60 (0^+) and 85 (2^+) which are located in the region of $\epsilon_{nI} < 25$ MeV. For 18-MeV scattering, to take pseudo-states of $\epsilon_{nI} < 12$ MeV is satisfactory. The case (b) was found to be sufficient to obtain a good convergence.

$$\times \Big[[Y_\lambda(\hat{\mathbf{y}}_c) \otimes Y_\ell(\hat{\mathbf{r}}_c)]_\Lambda \otimes [\eta_{\frac{1}{2}}^{(n_1)} \otimes \eta_{\frac{1}{2}}^{(n_2)}]_S \Big]_{Im}, \tag{3.2}$$

where λ (ℓ) is the angular momentum regarding the Jacobian coordinates $\mathbf{y}_c$ ($\mathbf{r}_c$), and $\eta_{1/2}$ is the spin wave function of each valence neutron (n_1 or n_2). ^{4}He has been treated as an inert core with the $(0s)^4$ internal configuration, $\varphi^{(\alpha)}$. The Gaussian range parameters are taken to lie in geometric progression:

$$\bar{y}_i = \bar{y}_1 (\bar{y}_{\max}/\bar{y}_1)^{(i-1)/(i_{\max}-1)}, \tag{3.3}$$

$$\bar{r}_j = \bar{r}_1 (\bar{r}_{\max}/\bar{r}_1)^{(j-1)/(j_{\max}-1)}. \tag{3.4}$$

Φ_{nIm} is antisymmetrized for the exchange between n_1 and n_2. Meanwhile, the exchange between each valence neutron and each nucleon in ^{4}He is treated approximately by the

orthogonality condition. The eigenenergies ϵ_{nI} of ^{6}He and the corresponding expansion-coefficients $A^{(c)nI}_{i\lambda j\ell\Lambda S}$ are determined by diagonalizing the Hamiltonian of the interrenal motion of ^{6}He [14, 15] using a large number of three-body Gaussian basis functions. Detailed information on the basis is listed in Ref.[4]. The calculated ϵ_{nI} are -0.98 MeV for the 0^+ ground state and 0.72 MeV for the 2^+ resonance state; here, we took the Bonn A potential between the valence nucleons and increased the depth of the $n-\alpha$ potential by a few percent so that the ground-state energy is reproduced.

In the four-body CDCC calculation of ^{6}He+^{12}C shown in a later section, we take $I^\pi = 0^+$ and 2^+ states for ^{6}He. Here we omit the 1^- state that does not contribute to the nuclear breakup processes (but they are included in the calculation of Coulomb and nuclear breakup in Ref.[7]). In order to demonstrate the convergence of the four-body CDCC solution with increasing the number of the Gaussian basis functions, we prepare three sets of the basis functions, i.e., sets I, II and III listed in Table II of [4]. Resultant energy levels of the ground and pseudo-states are shown in (a), (b) and (c) in Fig. 8, respectively. For ^{6}He+^{12}C scattering at 18 MeV (229.8 MeV) which will be discussed in the next section, high-lying states with $\epsilon_{nI} > 12$ MeV ($\epsilon_{nI} > 25$ MeV) are found to give no effect on the elastic and breakup S-matrix elements. Thus, the effective number of the eigenstates of ^{6}He, is reduced much for each of cases (a), (b), (c) as shown in Fig. 8. The case (b) was found to be sufficient to obtain a good convergence. In the GEM, computation time to obtain the wave functions of the bound and pseudo states is very short; for example, all the wave functions of the states in Fig. 8(c) is obtained in 10 minutes on FUJITSU VPP5000, a supercomputer.

It is to be noted that the bound and pseudo-states obtained with the GEM calculations construct an approximate complete sets for each $J(= 0, 1, 2)$ in a finite region which is responsible for the reaction; this was examined by checking that those states (below 100 MeV) satisfies 99.9 % of the energy-weighted cluster sum-rule limit for monopole, dipole and quadrupole transitions.

IV. FOUR-BODY CDCC ANALYSIS OF ^{6}He+^{12}C SCATTERING AT 18 AND 229.8 MEV

In this section, we briefly introduce the results obtained in the work of Ref.[4]. We performed the four-body CDCC calculation for ^{6}He+^{12}C scattering at 18 and 229.8 MeV using the wave functions of the bound state and the pseudo-states of ^{6}He obtained above.

The real part of the CC potentials, say $V^J_{nIL,n'I'L'}(R)$, was constructed by using the double-folding model [18]; the potentials were calculated by folding the DDM3Y NN interaction into the transition densities between the states $\Phi_{nI}(\xi)$ and $\Phi_{n'I'}(\xi)$ (cf. Ref.[4] for details) and the ground-state density of ^{12}C [19] . The imaginary part was assumed, as usually done [1], to be given as (together with the real part)

$$(N_R + iN_I)\, V^J_{nIL,n'I'L'}(R), \tag{4.1}$$

where $N_R = 1.0$ with no renormarization of the real part. The only parameter N_I is searched

for to reproduce the observed elastic cross section as well as possible. In the analysis of the ^{6}He+^{12}C scattering, Coulomb breakup effect is ignored since it is negligible for this light target; the Coulomb potential is assumed to work between the center-of-mass of the target and that of the projectile.

Calculated and observed elastic cross sections for ^{6}He+^{12}C scattering at 18 MeV are shown in Fig. 9. The optimum value of N_I is 0.5, which is the same as that for ^{6}Li scattering at various incident energies [1]. The dotted lines represent the elastic cross sections due to the single-channel calculation. Then, the difference between the solid and dotted lines shows the effect of the four-body breakup on the elastic cross section. The effect is sizable and indispensable to explain the behavior of the angular distribution. The case at 229.8 MeV is shown in Fig.10 and the optimum value of N_I is 0.3. The breakup effect in this case is also important in reproducing the data. The origin of the small N_I value for the ^{6}He scattering at 229.8 MeV is not clear at this moment, so more systematic experimental data are highly desirable for ^{6}He scattering.

We calculated the dynamical polarization (DP) potential induced by the four-body breakup processes, in order to understand effects of the processes on the elastic scattering. The DP potential is given by the deviation of the so-called wave-function-equivalent local potential derived using the elastic channel amplitude in the solution of the CDCC equation from the double-folding potential of the elastic channel. From the analysis [4] of the DP potential, one sees that inclusion of the four-body breakup processes makes the real part of the ^{6}He–^{12}C potential shallower and the imaginary one deeper compared with the double-folding potential of the elastic channel. In particular, the latter effect is important and can be assumed to come from the Borromean structure of ^{6}He. This is consistent with the fact that the total reaction cross section is enhanced by the Borromean structure[4].

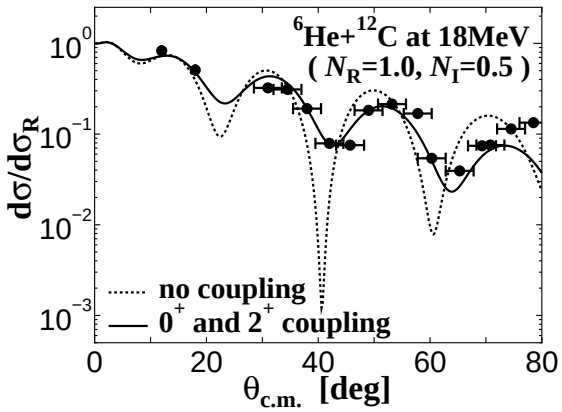

FIG. 9: Angular distribution of the elastic differential cross section for ^{6}He+^{12}C scattering at 18 MeV. The solid and dotted lines show the results with and without breakup effects, respectively. The experimental data are taken from Ref. [17]. This figure is taken from [4].

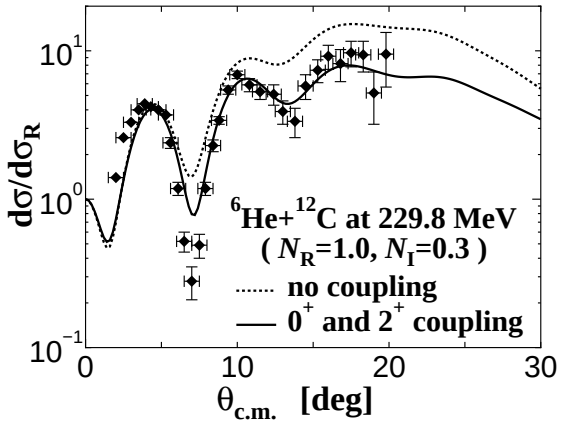

FIG. 10: The same as in Fig. 9 but for ^{6}He+^{12}C scattering at 229.8 MeV. The experimental data are taken from Ref. [16]. This figure is taken from [4].

V. CONCLUSION AND NEAR-FUTURE PROBLEMS

In conclusion, a fully quantum-mechanical method of treating four-body breakup is presented by extending CDCC. The validity of the method called four-body CDCC is confirmed by clear convergence of the calculated elastic and energy-integrated breakup cross sections with respect to extending the modelspace. The four-body CDCC is found to explain well the ^{6}He+^{12}C scattering at 18 and 229.8 MeV in which ^{6}He easily breaks up into two neutrons and ^{4}He. For the elastic scattering, the four-body breakup processes make, in particular, the imaginary part of the ^{6}He–^{12}C potential deeper, which is originated in the Borromean structure of ^{6}He.

In the analysis of [4], four-body Coulomb breakup is neglected. However, it is possible to treat it within the four-body CDCC framework (cf. Fig. 1). Actually, after this RIA workshop, we reported in Ref.[7] our four-body CDCC calculation of the ^{6}He+^{209}Bi scattering at 19.0 and 22.5 MeV taking both the Coulomb and nuclear breakup effects into account. The elastic cross sections were well reproduced by the calculation. So, the same framework will be applicable to other cases of three-body projectiles with Coulomb and nuclear breakup.

In order to treat both Coulomb and nuclear breakup processes at *intermediate energies*, Ref. [6] proposed a new method, namely a hybrid calculation with the three-body CDCC method and the eikonal-CDCC (E-CDCC) method. This hybrid calculation is expected to be opening the door to the systematic analysis of Coulomb (plus nuclear) dissociation of projectiles in the wide range of beam energies. For example, the method was recently applied to the analysis of ^{8}B dissociation measurements to determine the astrophysical factor $S_{17}(0)$ accurately [20].

There are some important unstable nuclei that are considered to be composed of four-body constituents. For reactions in which such a four-body nucleus is a projectile, a five-body CDCC calculation is required. The GEM was already severely and successfully tested for the bound states and pseudo-states of four-body systems. A good example is seen in a calculation of four-nucleon system (^{4}He) in Ref. [21]. The four-body GEM calculation with a realistic

NN force (AV8') and a phenomenological NNN force (which is adjusted to reproduce the ground-state energy) reproduced the energy of the second 0^+ state and the ^{4}He$(e,e')^4$He(0_2^+) form factor. Furthermore, some 3000 0^+ pseudo-states below 300-MeV excitation satisfied the energy-weighted monopole sum rule by 99.9% (with saturation) and made clear, for the first time, that the major part of the monopole sum rule limit, which had been long unknown, was distributed into low-lying four-body non-resonant continuum states. So, it may be said that it is ready to perform five-body CDCC calculations for reactions induced by four-body projectiles.

---

[1] M. Kamimura, M. Yahiro, Y. Iseri, Y. Sakuragi, H. Kameyama and M. Kawai, Prog. Theor. Phys. Suppl. **89**, 1 (1986).

[2] For a review, E. Hiyama, Y. Kino and M. Kamimura, Prog. Part. Nucl. Phys. **51**, 223 (2003).

[3] T. Matsumoto, T. Kamizato, K. Ogata, Y. Iseri, E. Hiyama, M. Kamimura and M. Yahiro, Phys. Rev. C **68**, 064607 (2003).

[4] T. Matsumoto, E. Hiyama, K. Ogata, Y. Iseri, M. Kamimura, S. Chiba and M. Yahiro, Phys. Rev. C **70**, 061601 (R)(2004).

[5] T. Egami, K. Ogata, T. matsumoto, Y. Iseri, M. Kamimura and M. Yahiro, Phys. Rev. C **70** 047604 (2004).

[6] K. Ogata, M. Yahiro, Y. Iseri, T. Matsumoto and M. Kamimura, Phys. Rev. C **68** 064609 (2003).

[7] T. Egami, T. Matsumoto, K. Ogata, Y. Iseri, M. Kamimura, E. Hiyama and M. Yahiro, a talk at Annual Meeting of Japan Physical Society, March, 2005, Noda.

[8] A. M. Moro, J. M. Arias, J. Gómez-Camacho, I. Martel, F. Pérez-Bernal, R. Crespo and F. Nunes, Phys. Rev. C **65**, 011602 (2002).

[9] R. Y. Rasoanaivo and G. H. Rawitscher, Phys. Rev. C **39**, 1709 (1989).

[10] M. Kamimura, Phys. Rev. A **38**, 621 (1988).

[11] Particle Data Group, D. E. Groom *et al.*, Eur. Phys. J. **C15**, 1 (2000).

[12] H.A. Torii *et al.*, Phys. Rev. A59 (1999) 223.

[13] Y. Kino, M. Kamimura and H. Kudo, Hyperfine Interact., **119**, 201 (1999).

[14] S. Funada *et al.*, Nucl. Phys. **A575**, 93 (1994).

[15] E. Hiyama and M. Kamimura, Nucl. Phys. **A588**, 35 (1995).

[16] V. Lapoux *et al.*, Phys. Rev. C **66**, 034608 (2002).

[17] M. Milin *et al.*, Nucl. Phys. **A730**, 285 (2004).

[18] G. R. Satchler and W. G. Love, Phys. Rep. **55**, 183 (1979).

[19] M. Kamimura, Nucl. Phys. **A351**, 456 (1981).

[20] K. Ogata, S. hashimoto, Y. Iseri, M. Kamimura and M. Yahiro, nucl-th/0505007 (2005).

[21] E. Hiyama, B.F. Gibson and M. Kamimura, Phys. Rev. C **70**, 031001(R) (2004).